


# Importance of Out-of-State Spin–Orbit Coupling for Slow Magnetic Relaxation in Mononuclear Fe<sup>II</sup> Complexes

Po-Heng Lin,<sup>†,‡</sup> Nathan C. Smythe,<sup>§</sup> Serge I. Gorelsky,<sup>†,‡</sup> Steven Maguire,<sup>†,‡</sup> Neil J. Henson,<sup>⊥</sup> Ilia Korobkov,<sup>†</sup> Brian L. Scott,<sup>||</sup> John C. Gordon,<sup>§</sup> R. Tom Baker,<sup>†,‡</sup> and Muralee Murugesu<sup>\*,†,‡</sup>

<sup>†</sup>Department of Chemistry and <sup>‡</sup>Centre for Catalysis Research and Innovation, University of Ottawa, Ottawa, Ontario K1N 6N5, Canada

<sup>§</sup>Chemistry Division, <sup>⊥</sup>Theoretical Division, and <sup>||</sup>Materials Physics and Applications Division, Los Alamos National Laboratory, MS J582, Los Alamos, New Mexico 87545, United States

 Supporting Information

**ABSTRACT:** Two mononuclear high-spin Fe<sup>II</sup> complexes with trigonal planar ([Fe<sup>II</sup>(N(TMS)<sub>2</sub>)<sub>2</sub>(PCy<sub>3</sub>)] (1) and distorted tetrahedral ([Fe<sup>II</sup>(N(TMS)<sub>2</sub>)<sub>2</sub>(depe)] (2) geometries are reported (TMS = SiMe<sub>3</sub>, Cy = cyclohexyl, depe = 1,2-bis(diethylphosphino)ethane). The magnetic properties of 1 and 2 reveal the profound effect of out-of-state spin–orbit coupling (SOC) on slow magnetic relaxation. Complex 1 exhibits slow relaxation of the magnetization under an applied optimal dc field of 600 Oe due to the presence of low-lying electronic excited states that mix with the ground electronic state. This mixing re-introduces orbital angular momentum into the electronic ground state via SOC, and 1 thus behaves as a field-induced single-molecule magnet. In complex 2, the lowest-energy excited states have higher energy due to the ligand field of the distorted tetrahedral geometry. This higher energy gap minimizes out-of-state SOC mixing and zero-field splitting, thus precluding slow relaxation of the magnetization for 2.

In discrete molecular complexes, the combination of non-negligible spin ground state *S* and uniaxial Ising-like anisotropy  $|D|$  (taking into account the Hamiltonian,  $H = DS_z^2$ ) gives rise to an energy barrier *U*, defined as  $S^2|D|$  and  $(S^2 - 1/4)|D|$  for integer and half-integer spins, respectively. Molecules with significant *U* values exhibit slow relaxation of their magnetization, indicating magnet-like behavior,<sup>1</sup> and are termed single-molecule magnets (SMMs).<sup>1,2</sup> In an effort to increase the energy barrier in SMMs for application purposes, much effort has been focused on obtaining high-spin (HS) systems, without much success.<sup>3</sup> Therefore, in recent years many research groups have dedicated their efforts toward controlling magnetic anisotropy ( $|D|$ ) by looking to highly anisotropic metal ions.<sup>4</sup>

Magnetic anisotropy can be introduced into complexes with unpaired electrons through structural distortions (such as Jahn–Teller splitting) and spin–orbit coupling (SOC) involving one or more electronic states.<sup>1,5</sup> Two SOC effects can be present: (a) SOC that involves an orbitally degenerate electronic ground state, and (b) SOC that involves an orbitally non-degenerate ground state with low-lying electronic excited states. Typical examples of the first case are d<sup>n</sup> metal ion complexes with coordination geometries that allow orbital degeneracy. For instance, in an octahedral HS d<sup>6</sup> complex, the partially filled t<sub>2g</sub>

levels are degenerate, as the d<sub>xy</sub>, d<sub>xz</sub>, and d<sub>yz</sub> orbitals can be inter-converted by a rotation of 90° about the *x*-, *y*-, or *z*-axis. Thus, in the ground state of these complexes, the orbital angular momentum is not quenched by the ligand field, and the resulting strong “in-state” SOC can give rise to a sizable axial zero-field-splitting (ZFS) parameter,  $|D|$ .<sup>1,5</sup> In contrast, octahedral HS Mn<sup>III</sup> complexes are an example of “out-of-state” SOC systems. These complexes have an orbitally non-degenerate electronic state, and, as a result, in-state SOC cannot contribute to nonzero ZFS. However, SOC of the non-degenerate ground state with low-lying excited states bearing angular momenta can produce ZFS. Thus, SOC has a profound effect on the magnetic properties of molecular complexes.<sup>1</sup>

To fully understand magnetic anisotropy effects on slow magnetic relaxation, it is important to investigate structurally simple molecules that exhibit SOC. In order to assess how significant out-of-state SOC contributions can be to ZFS, we focused our attention on mononuclear HS Fe<sup>II</sup> complexes with ligand fields that produce structures with non-degenerate ground states. Herein we report the synthesis of three- and four-coordinate mononuclear Fe<sup>II</sup> complexes, each containing two bis(trimethylsilyl)amide ligands along with monodentate tricyclohexylphosphine (PCy<sub>3</sub>) or bidentate 1,2-bis(diethylphosphino)ethane (depe) ligands. Detailed magnetic studies reveal significant differences in the magnetic behavior of these three- and four-coordinate complexes due to the difference in their electronic structures arising from the disparate Fe coordination geometries.

The planar three-coordinate complex [Fe<sup>II</sup>(N(TMS)<sub>2</sub>)<sub>2</sub>(PCy<sub>3</sub>)] (1) was obtained from the reaction of PCy<sub>3</sub> and FeCl<sub>2</sub> (1:1) in THF, followed by addition of potassium bis(trimethylsilyl)amide (KN(TMS)<sub>2</sub>) (2 equiv) at –25 °C. The detailed synthetic procedure can be found in the Supporting Information. Complex 1 crystallizes in the monoclinic space group *P*2<sub>1</sub>/*n* as a mononuclear Fe<sup>II</sup> complex (Figure 1, left). The central Fe<sup>II</sup> ion is coordinated by one PCy<sub>3</sub> and two N(TMS)<sub>2</sub> ligands in a trigonal planar arrangement (sum of angles, 359.9°). The coordinated N1, N2 atoms (Fe–N (1.95 Å)) and the P1 atom (Fe–P (2.52 Å)) form a planar near isosceles triangle wherein the Fe<sup>II</sup> center lies only 0.03 Å above the plane. The N1–Fe–N2 angle of 128.5° leads to a small distortion that can be seen in the N1–Fe–P1 and N2–Fe–P1 angles of 115.2° and 116.3°, respectively. A close inspection of the packing arrangement reveals layered ABAB

Received: April 26, 2011

Published: September 06, 2011

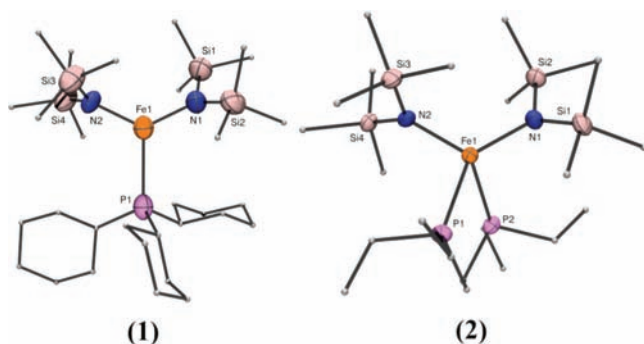


**Figure 1.** Molecular structures of (left) the three-coordinate complex  $[\text{Fe}^{\text{II}}(\text{N}(\text{TMS})_2)_2(\text{PCy}_3)]$  (**1**) and (right) the four-coordinate complex  $[\text{Fe}^{\text{II}}(\text{N}(\text{TMS})_2)_2(\text{depe})]$  (**2**). Hydrogen atoms and carbon atom labels have been omitted for clarity.

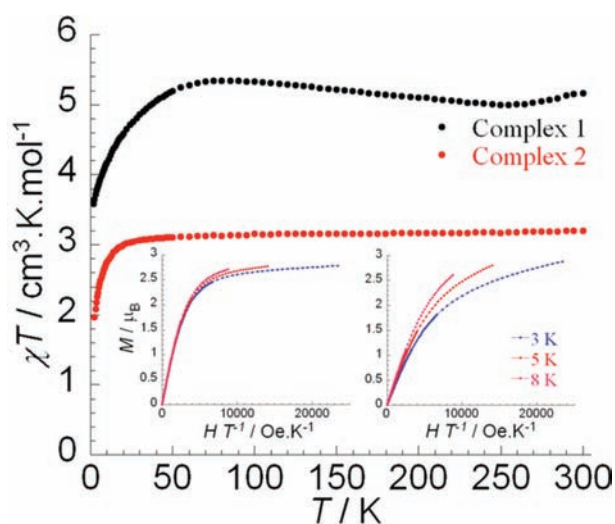


**Figure 2.** Temperature dependence of  $\chi T$  at 1000 Oe for **1** and **2**. Inset:  $M$  vs  $H/T$  plots at 3, 5, and 8 K for **1** (left) and **2** (right).

packing along the crystallographic  $c$ -axis (Figure S1), with the shortest  $\text{Fe} \cdots \text{Fe}$  distance of 9.53 Å between adjacent molecules. It is noteworthy that **1** joins a rare family of other reported three-coordinate Fe complexes.<sup>6</sup> As a consequence of its low coordination geometry and +2 oxidation state, **1** is extremely reactive and readily oxidizes upon exposure to air. The four-coordinate complex  $[\text{Fe}^{\text{II}}(\text{N}(\text{TMS})_2)_2(\text{depe})]$  (**2**) was obtained from the reaction of  $\text{LiN}(\text{TMS})_2$  and  $\text{FeBr}_2$  (2:1) in THF at  $-25$  °C, followed by addition of *depe* (1 equiv). Complex **2** crystallizes in the tetragonal space group  $P4_1$  as a mononuclear  $\text{Fe}^{\text{II}}$  complex (Figure 2, right). The coordination environment of the  $\text{Fe}^{\text{II}}$  center reveals a distorted tetrahedral geometry with a  $\text{P1}-\text{Fe}-\text{P2}$  angle of  $78.4^\circ$  and an  $\text{N1}-\text{Fe}-\text{N2}$  angle ( $120.9^\circ$ ) that is significantly smaller than that of **1** ( $128.5^\circ$ ). The shortest  $\text{Fe} \cdots \text{Fe}$  distance of 10.04 Å between adjacent molecules is shown in the packing arrangement along the  $a$ -axis (Figure S2). Such large separation distances are generally inefficient for intermolecular magnetic interactions. A comparison of selected bond distances and angles for **1** and **2** is presented in Table 1, and further structural information is given in Figures S3 and S4 and Tables S1–S11.

Magnetic studies were carried out on powdered polycrystalline samples of **1** and **2** prepared in a glovebox. Both mononuclear

**Table 1.** Selected Bond Lengths (Å) and Angles ( $^\circ$ ) of **1** and **2**

	<b>1</b>	<b>2</b>	<b>1</b>	<b>2</b>
Fe–N1	1.95	1.99	Fe–P1	2.52
Fe–N2	1.95	1.99	Fe–P2	2.59
N1–Fe–N2	128.5	120.9	P1–Fe–P2	78.4
N1–Fe–P1	115.2	129.1	N1–Fe–P2	99.2
N2–Fe–P1	116.3	98.3	N2–Fe–P2	126.2

$\text{Fe}^{\text{II}}$  complexes exhibited clearly distinct magnetic behavior under direct current (dc) and alternating current (ac) measurements. At room temperature,  $\chi T$  values of  $5.16$  and  $3.20 \text{ cm}^3 \cdot \text{K} \cdot \text{mol}^{-1}$  for **1** and **2**, respectively, were obtained (Figure 2). The latter value for **2** is in good agreement with the expected theoretical spin-only value of  $3 \text{ cm}^3 \cdot \text{K} \cdot \text{mol}^{-1}$  for a non-interacting HS  $\text{Fe}^{\text{II}}$  ion ( $S = 2$ ,  $g = 2$ ,  $\chi T = g^2 S(S + 1)/8$ ). Conversely, the observed  $\chi T$  value for **1** is much higher than the expected spin-only value. This can be attributed to the presence of a significant orbital contribution in **1**, which makes the spin-only formula invalid for a HS  $d^6$  ion. Therefore, it is important to take the orbital contribution into account. The observed  $\chi T$  value of  $5.16 \text{ cm}^3 \cdot \text{K} \cdot \text{mol}^{-1}$  is close to the expected value of  $5.6 \text{ cm}^3 \cdot \text{K} \cdot \text{mol}^{-1}$  for an  $\text{Fe}^{\text{II}}$  ( $^5D_4$ ,  $S = 2$ ,  $L = 2$ ,  $J = 4$ ,  $g = 3/2$ ,  $\chi T = g^2 J(J + 1)/8$ ) ion with unquenched orbital angular momentum.<sup>7</sup> Similar observations have been reported by Reiff et al. for a two-coordinate HS  $\text{Fe}^{\text{II}}$  complex with significant SOC.<sup>5c,d</sup>

Upon lowering the temperature, the  $\chi T$  product remains constant until 20 K for **2**, whereas for **1**, the  $\chi T$  product initially decreases slightly before increasing back to  $5.3 \text{ cm}^3 \cdot \text{K} \cdot \text{mol}^{-1}$ . Overall, this slight variation of the  $\chi T$  product for **1** is in the  $5.0$ – $5.3 \text{ cm}^3 \cdot \text{K} \cdot \text{mol}^{-1}$  range. At temperatures below 50 K for **1** and 20 K for **2**, a rapid decrease in  $\chi T$  can be observed with minimum values of  $3.59$  and  $1.97 \text{ cm}^3 \cdot \text{K} \cdot \text{mol}^{-1}$  at 2 K for **1** and **2**, respectively. Complex **2** clearly obeys the expected Curie–Weiss-type behavior ( $c = 3.21 \text{ cm}^3 \cdot \text{K} \cdot \text{mol}^{-1}$ ;  $\theta = -1.64$ ) (Figure S5), whereas the origin of the observed slight inflection for **1** remains unclear. In the latter case, a physical torquing effect can be ruled out, as the data are highly reproducible even under different restraining matrices such as grease or eicosane. Single-crystal X-ray studies reveal that the geometries of **1** at low (120 K) and high (298 K) temperatures are nearly identical, and no spin crossover or phase transition is observed. Although the intermolecular distances are significant, the low-temperature decrease of the  $\chi T$  product could also be due to very weak antiferromagnetic interactions for **1** and **2**. The more pronounced decrease in **1** also suggests the presence of significant ZFS due to its trigonal planar geometry (*vide infra*). To estimate the axial ZFS parameter ( $D$ ), fitting of the susceptibility data assuming a simple ZFS effect was carried out (Figure S6).<sup>8</sup> An excellent fit was obtained for **1** (below 50 K) and **2** (2–300 K range), with  $D$  values of  $-10.9$  and  $+5.9$  K, respectively.

The field dependence of the magnetization of **1** and **2** below 8 K is shown in Figures 2 (inset), S7, and S8. The lack of saturation and non-superposition on a single master curve of  $M$  vs  $H/T$  data also suggests the presence of low-lying excited states (for **1** and **2**) and magnetic anisotropy (for **1**) (*vide infra*). Several attempts to fit the reduced magnetization data using the Magnet<sup>9</sup> program were unsuccessful, most likely due to low-lying excited states.

To probe possible SMM behavior in both complexes, studies on the temperature and frequency dependence of the ac susceptibility were carried out in the temperature range 2.2–15 K.

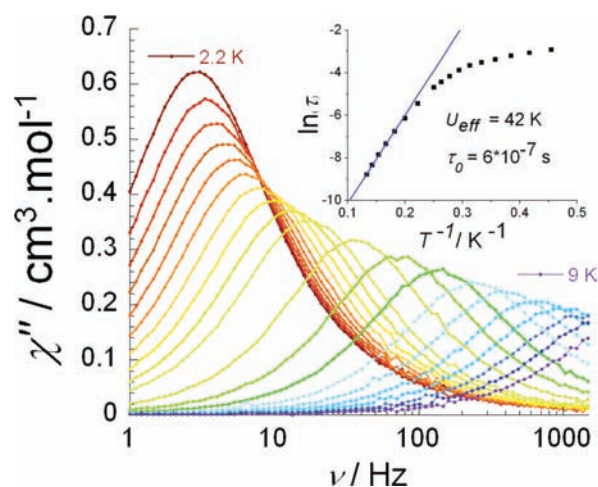


**Figure 3.** Out-of-phase susceptibility ( $\chi''$ ) vs frequency  $\nu$  (logarithmic scale) for **1** in the temperature range 2.2–9 K under an applied optimum dc field of 600 Oe. Inset: Relaxation time of the magnetization  $\ln(\tau)$  vs  $T^{-1}$  (Arrhenius plot using ac data). The solid line corresponds to the fit.

Under a zero dc field and a 3 Oe ac field oscillating at frequencies between 1 and 1500 Hz, no ac signal was observed. When a static dc field was applied, a frequency-dependent signal was observed only for **1** (Figures 3, S9–S11). Such behavior generally indicates that slow relaxation of the magnetization is highly influenced by quantum tunneling of the magnetization (QTM). This is most likely due to the presence of rhombic anisotropy ( $E$ ), causing the mixing of the  $\pm 2$  levels with the  $\pm 1$  level, subsequently providing the QTM pathway. Applying a static dc field will reduce QTM through the spin reversal barrier via degenerate  $\pm M_s$  energy levels; therefore, measurements at various applied dc fields will lift the degeneracy.<sup>2g</sup> To shortcut the tunneling effect, we initially carried out ac measurements under various dc fields to determine the optimum field for which the QTM is minimized (Figures S12 and S13). Ac measurements under the applied optimum field of 600 Oe reveal a frequency-dependent signal (Figures 3 and S11) with a clear out-of-phase ( $\chi''$ ) peak. Such behavior is indicative of super-paramagnet-like slow magnetization relaxation of a SMM. An anisotropic energy barrier ( $U_{\text{eff}}$ ) can be obtained from the high-temperature regime of the slow magnetization relaxation where it is thermally induced (Arrhenius law,  $\tau = \tau_0 \exp(U_{\text{eff}}/kT)$ ). The obtained value of  $U_{\text{eff}} = 42$  K ( $\tau_0 = 6 \times 10^{-7}$  s) (Figure 3 inset) is close to that previously reported for the trigonal pyramidal  $[(\text{tpaMes})\text{Fe}]^-$  complex by Long, Chang, and co-workers.<sup>5b</sup> By using the  $U = S^2|D|$  equation and the obtained  $U_{\text{eff}}$  value, we can deduce that  $D \approx 10$  K. A single relaxation mechanism can be confirmed by fitting the Cole–Cole plot (Figure S14), and the obtained fits ( $\alpha = 0.03$ – $0.1$ ) using the Debye model<sup>1b</sup> are in good agreement with such behavior.

To further investigate the electronic structure of these molecules, and to understand why the SMM properties are only present in the case of **1**, nonrelativistic density functional theory (DFT) calculations were carried out. Geometry optimization calculations were performed on models of the molecular species constructed using the crystal structure data as starting points and employing the spin-unrestricted formalism to assess the effect of differing spin states at the PBE<sup>10</sup>/TZVP<sup>11</sup> level of theory. The calculations were also repeated at the B3LYP<sup>12</sup>/TZVP level of theory to confirm the results and to assess the sensitivity of the results to the exchange-correlation potential (*vide infra*). For

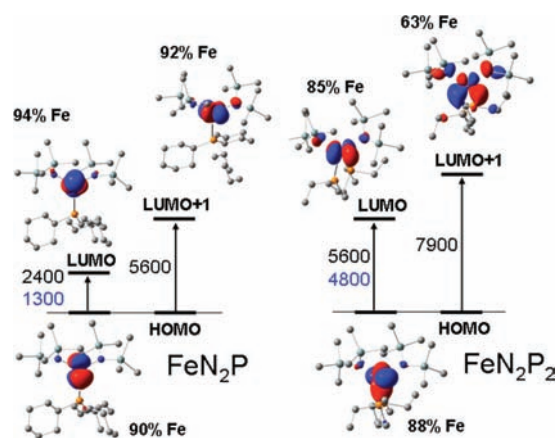


**Figure 4.** TD-DFT calculated two lowest-energy excited states and the  $\beta$ -spin molecular orbitals involved in the excitations for **1** (left) and **2** (right). The excited-state energies ( $\text{cm}^{-1}$ ) from PBE and B3LYP calculations are shown in black and blue, respectively. The percent contributions of the Fe atom to the density of molecular orbitals are also shown. H atoms are omitted for clarity.

both **1** and **2**, the lowest energy  $d^6$  spin state is predicted to be HS (quintet vs singlet and triplet). The HS structures reproduce the experimental bond lengths and angles closely. Selected geometric parameters are shown in Table S12 for the optimized geometries. In the quintet state, most of the spin density is localized on the  $\text{Fe}^{\text{II}}$  center (NPA<sup>13</sup>-derived atomic spin density is 3.46 for **1** and 3.40 for **2**). The calculated Mayer bond orders<sup>14,15</sup> for Fe–P and Fe–N bonds are 0.69 and 0.82 in **1** and 0.51–0.55 and 0.75–0.77 in **2**, respectively. Thus, the metal–ligand bonds in **1** carry more covalency<sup>15</sup> than the metal–ligand bonds in **2** to compensate for the lower coordination number in **1**. Overall, the NPA-derived atomic charges of the  $\text{Fe}^{\text{II}}$  center (+0.96 au in **1** and +0.73 au in **2**) indicate that this compensation through higher metal–ligand covalency was not quite complete, and, as a result, the d orbital splitting due to metal–ligand interactions in **1** can be expected to be lower than in **2**. Time-dependent DFT (TD-DFT)<sup>16</sup> calculations were used to calculate the energies of the lowest-energy excited states for **1** and **2**. TD-DFT calculations performed using the hybrid B3LYP functional are in agreement with the TD-DFT calculations performed using the PBE functional (Figure 4).

Electronic transitions from the ground electronic state to four lowest-energy quintet excited states of the complexes are d–d (ligand-field)<sup>17</sup> excitations from the  $\beta$ -spin highest occupied molecular orbital (HOMO) to four  $\beta$ -spin lowest unoccupied molecular orbitals (LUMOs) (Figure 4 and S15).

Due to trigonal planar geometry, **1** has the  $\text{Fe } d_{xz}$  orbital (see Figure S16 for the orientation of the Cartesian axes with respect to the molecular frames) as the  $\beta$ -spin HOMO (Figure 4 left) and two excited states with very low energies ( $\sim 2000$   $\text{cm}^{-1}$  for the first excited state ( $d_{y^2-z^2}$ ) and  $\sim 5000$   $\text{cm}^{-1}$  for the second excited state ( $d_{yz}$ )). The two excited states that originate from the electron excitations from the  $\beta$ -spin HOMO to the remaining unoccupied Fe d orbitals have energies in the 10 000–14 000  $\text{cm}^{-1}$  range (Figure S15). Complex **2**, with its distorted tetrahedral geometry, has the  $d_{x^2-y^2}$  orbital as the  $\beta$ -spin HOMO (Figure 4 right), and the two lowest excited states have significantly higher energies ( $\sim 5000$   $\text{cm}^{-1}$  for the first excited state ( $d_{yz}$ ) and  $\sim 8000$   $\text{cm}^{-1}$  for the second excited state ( $d_{xy}$ )) than the two

lowest excited states in **1**. Since neither structure contains a three- or four-fold symmetry axis and the orbital energy levels in these systems are not degenerate, in-state SOC cannot be present. Only out-of state SOC can contribute to nonzero ZFS. The increase of the energies of the two lowest-energy excited states when going from **1** to **2** should significantly decrease the out-of-state SOC contribution to the ZFS. Indeed, no ac signal was observed for **2**, even under an applied field, indicating absence of slow relaxation of the magnetization. This is consistent with quenched orbital angular momentum and weak out-of-state SOC in a distorted tetrahedral Fe<sup>II</sup> complex. We can conclude that the remarkable observation of slow relaxation of the magnetization of **1** proves that it behaves as a field-induced SMM due to the large intrinsic magnetic anisotropy arising from out-of-state SOC in the trigonal planar complex.

The results described herein demonstrate that slow relaxation of the magnetization in **1** arises from the intrinsic magnetic anisotropy of the HS Fe<sup>II</sup> ion within a three-coordinate environment. This gives rise to very low-lying excited states that couple with the non-degenerate ground state via out-of-state SOC. The related four-coordinate complex, **2**, has a non-degenerate ground state and excited states with higher energies; thus, it does not exhibit magnetic anisotropy. We can conclude that out-of-state spin-orbit coupling for systems with low-lying excited states appear to be an important contributor to the slow magnetic relaxation of mononuclear complexes. We believe this may provide new avenues for conceiving polynuclear high-energy-barrier SMMs.

## ■ ASSOCIATED CONTENT

**S** **Supporting Information.** Complete experimental and computational details (PDF); X-ray crystallographic files (CIF). This material is available free of charge via the Internet at <http://pubs.acs.org>.

## ■ AUTHOR INFORMATION

**Corresponding Author**  
m.murugesu@uottawa.ca

## ■ ACKNOWLEDGMENT

We thank the University of Ottawa (start-up), CCRI, CFI, FFCR, NSERC (Discovery and RTI grants), ERA, and U.S. DOE Office of Energy Efficiency and Renewable Energy for their support.

## ■ REFERENCES

- (1) (a) Kahn, O. *Molecular Magnetism*; VCH-Wiley: New York, 1993. (b) Gatteschi, D.; Sessoli, R.; Villain, J. *Molecular Nanomagnets*; Oxford University Press: New York, 2006.
- (2) (a) Christou, G.; Gatteschi, D.; Hendrickson, D. N.; Sessoli, R. *MRS Bull.* **2000**, *25*, 66. (b) Thomas, L.; Lioni, L.; Ballou, R.; Gatteschi, D.; Sessoli, R.; Barbara, B. *Nature* **1996**, *383*, 145. (c) Sokol, J. J.; Hee, A. G.; Long, J. R. *J. Am. Chem. Soc.* **2002**, *124*, 7656. (d) Maheswaran, S.; Chastanet, G.; Teat, S. J.; Mallah, T.; Sessoli, R.; Wernsdorfer, W.; Winpenny, R. E. P. *Angew. Chem., Int. Ed.* **2005**, *44*, 5044. (e) Inglis, R.; Jones, L. F.; Karotsis, G.; Collins, A.; Parsons, S.; Perleps, S. P.; Wernsdorfer, W.; Brechin, E. K. *Chem. Commun.* **2008**, 5924. (f) Schelter, E. J.; Karadas, F.; Avendano, C.; Prosvirin, A. V.; Wernsdorfer, W.; Dunbar, K. R. *J. Am. Chem. Soc.* **2007**, *129*, 8139. (g) Li, D.; Clerac, R.; Parkin, S.; Wang, G.; Yee, G. T.; Holmes, S. M. *Inorg. Chem.* **2006**, *45*, 5251.
- (3) (a) Ako, A. M.; Hewitt, I. J.; Mereacre, V.; Clerac, R.; Wernsdorfer, W.; Anson, C. E.; Powell, A. K. *Angew. Chem., Int. Ed.* **2006**, *45*, 4926.

(b) Murugesu, M.; Habrych, M.; Wernsdorfer, W.; Abboud, K. A.; Christou, G. *J. Am. Chem. Soc.* **2004**, *126*, 4766. (c) Larionova, J.; Gross, M.; Pilkington, M.; Andres, H.; Stoeckli-Evans, H.; Gudel, H.; Decurtins, S. *Angew. Chem., Int. Ed.* **2000**, *39*, 1605.

(4) (a) Long, J.; Habib, F.; Lin, P.-H.; Korobkov, I.; Enright, G.; Ungur, L.; Wernsdorfer, W.; Chibotaru, L. F.; Murugesu, M. *J. Am. Chem. Soc.* **2011**, *133*, 5319. (b) Ishikawa, N.; Sugita, M.; Ishikawa, T.; Koshihara, S.; Kaizu, Y. *J. Am. Chem. Soc.* **2003**, *125*, 8694. (c) Petit, S.; Pilet, G.; Luneau, D.; Chibotaru, L. F.; Ungur, L. *Dalton Trans.* **2007**, 4582. (d) AlDamen, M. A.; Clemente-Juan, J. M.; Coronado, E.; Marti-Gastaldo, C.; Gaita-Arino, A. *J. Am. Chem. Soc.* **2008**, *130*, 8874. (e) Weismann, D.; Sun, Y.; Lan, Y.; Wolmershäuser, G.; Powell, A. K.; Sitzman, H. *Chem.—Eur. J.* **2011**, *17*, 4700.

(5) (a) Atanasov, M.; Ganyushin, D.; Pantazis, D. A.; Sivalingham, K.; Neese, F. *Inorg. Chem.* **2011**, *50*, 7460. (b) Freedman, D. E.; Harman, W. H.; Harris, T. D.; Long, G. J.; Chang, C. J.; Long, J. R. *J. Am. Chem. Soc.* **2010**, *132*, 1224. (c) Reiff, W. M.; LaPointe, A. M.; Witten, E. H. *J. Am. Chem. Soc.* **2004**, *126*, 10206. (d) Reiff, W. M.; Schulz, C. E.; Whangbo, M.-H.; Seo, J. L.; Lee, Y. S.; Potratz, G. R.; Spicer, C. W.; Girolami, G. S. *J. Am. Chem. Soc.* **2009**, *131*, 404.

(6) (a) Vela, J.; Smith, J. M.; Lachicotte, R. J.; Holland, P. L. *Chem. Commun.* **2002**, 2886. (b) Olmstead, M. M.; Power, P. P.; Shoner, S. C. *Inorg. Chem.* **1991**, *30*, 2547. (c) Siemeling, U.; Vorfeld, U.; Neumann, B.; Stammler, H.-G. *Inorg. Chem.* **2000**, *39*, 5159. (d) Chiang, K. P.; Barrett, P. M.; Ding, F.; Smith, J. M.; Kingsley, S.; Brennessel, W. W.; Clark, M. M.; Lachicotte, R. J.; Holland, P. L. *Inorg. Chem.* **2009**, *48*, 5106. (e) Vela, J.; Stoian, S.; Flaschenriem, C. J.; Munck, E.; Holland, P. L. *J. Am. Chem. Soc.* **2004**, *126*, 4522. (f) Zhang, Y.; Oldfield, E. *J. Phys. Chem. B* **2003**, *107*, 7180. (g) Gregory, E. A.; Lachicotte, R. J.; Holland, P. L. *Organometallics* **2005**, *24*, 1803. (h) Holland, P. L. *Acc. Chem. Res.* **2008**, *41*, 905. (i) Fitzsimmons, B. W.; Johnson, C. E. *Chem. Phys. Lett.* **1974**, *24*, 422. (j) Cowley, R. E.; DeYonker, N. J.; Eckert, N. A.; Cundari, T. R.; DeBeer, S.; Bill, E.; Ottenwaelder, X.; Flaschenriem, C.; Holland, P. L. *Inorg. Chem.* **2010**, *49*, 6172. (k) Pali, A. V.; Clemente-Juan, J. M.; Coronado, E.; Klokishner, S. I.; Ostrovsky, S. M.; Reu, O. S. *Inorg. Chem.* **2010**, *49*, 8073.

(7) Mabbs, F. E.; Machin, D. J. *Magnetism and Transition Metal Complexes*; Dover Publications: New York, 2008.

(8) Chirico, R. D.; Carlin, R. L. *Inorg. Chem.* **1980**, *19*, 3031.

(9) Davidson, E. R. *MAGNET*; Indiana University: Bloomington, IN, 1999.

(10) Perdew, J. P.; Burke, K.; Ernzerhof, M. *Phys. Rev. Lett.* **1997**, *78*, 1396.

(11) Schafer, A.; Huber, C.; Ahlrichs, R. *J. Chem. Phys.* **1994**, *100*, 5829.

(12) (a) Becke, A. D. *J. Chem. Phys.* **1993**, *98*, 5648. (b) Lee, C.; Yang, W.; Parr, R. G. *Phys. Rev. B* **1988**, *37*, 785.

(13) Reed, A. E.; Weinstock, R. B.; Weinhold, F. *J. Chem. Phys.* **1985**, *83*, 735.

(14) Mayer, I. *Int. J. Quantum Chem.* **1986**, *29*, 73.

(15) Gorelsky, S. I.; Basumallick, L.; Vura-Weis, J.; Sarangi, R.; Hedman, B.; Hodgson, K. O.; Fujisawa, K.; Solomon, E. I. *Inorg. Chem.* **2005**, *44*, 4947.

(16) Stratmann, R. E.; Scuseria, G. E.; Frisch, M. J. *J. Chem. Phys.* **1998**, *109*, 8218.

(17) Lever, A. B. P. *Inorganic Electronic Spectroscopy*; Elsevier: Amsterdam, 1984.